Journal of Molecular Catalysis A: Chemical 353–354 (2012) 171–177

Contents lists available at SciVerse ScienceDirect

Journal of Molecular Catalysis A: Chemical

journal homepage: www.elsevier.com/locate/molcata

Electronic effect of Na promotion for selective mono-*N*-alkylation of aniline with di-*iso*-propylamine by Pt/SiO_2 catalysts

Ken-ichi Shimizu[a,*], Katsuya Shimura[a], Kazuo Kato[b], Naoko Tamagawa[c], Masazumi Tamura[c], Atsushi Satsuma[c]

[a] *Catalysis Research Center, Hokkaido University, N-21, W-10, Sapporo 001-0021, Japan*
[b] *Japan Synchrotron Radiation Research Institute, 1-1-1 Kouto, Mikazuki-cho, Sayo-gun, Hyogo 679-5198, Japan*
[c] *Department of Molecular Design and Engineering, Graduate School of Engineering, Nagoya University, Nagoya 464-8603, Japan*

ARTICLE INFO

Article history:
Received 14 October 2011
Received in revised form
21 November 2011
Accepted 23 November 2011
Available online 2 December 2011

Keywords:
Amines
Cross-coupling
Platinum
Sodium
Electronic effect

ABSTRACT

Sodium promoted 5 wt.% Pt/SiO_2 catalysts with similar Pt particle size (2.9–3.5 nm) but with different Na loadings (Na/Pt ratio of 0–10) were prepared by a sequential impregnation method. The catalysts were well characterized by Pt L_3-edge XAFS (X-ray absorption fine structure), X-ray photoelectron spectroscopy (XPS), infrared (IR) study of CO adsorption. Their catalytic activity for mono-*N*-alkylation of aniline with iPr_2NH, as a test reaction for cross-coupling reaction of different amines, showed a volcano type dependence on the Na/Pt ratio. The catalyst with Na/Pt ratio of 2 showed the highest intrinsic activity. The Na/Pt ratio also affected the electronic states of the support oxide and Pt; the electron densities of Pt and surface oxygen atoms of support oxides increased with the Na/Pt ratio. From the structure–activity relationship, it is shown that the moderate electron densities of Pt and support oxygen atoms lead to the high catalytic activity. Kinetic studies suggest that the present reaction proceeds through a hydrogen-borrowing mechanism that begins with dehydrogenation of iPr_2NH as the rate-limiting step. Based on the mechanistic and structural results, origin of the promotional effect of Na on the catalytic activity of Pt/SiO_2 is discussed.

1. Introduction

Supported metal catalysts play an important role in many heterogeneous catalytic reactions for green organic synthesis. Recent advances in synthetic catalysis established that supported Au, Ru, Rh, Pd, and Ag catalysts catalyze one-pot multi-step organic reactions, which provides a key technology for the green synthesis of fine chemicals [1–4]. Supported Pt metal nanoparticles have been the most industrially relevant and widely investigated catalysts [5–15] and several successful examples have demonstrated Pt-catalyzed green organic reactions such as hydrogenation [5,6] and selective oxidation of alcohols and sugars [7,8]. However, their applications to multi-step one-pot organic synthesis are limited. For developing a new catalyst for the organic synthesis, a fine control of the electronic state of metal centers in organometallic catalysts has been one of the most important design concepts. In the case of supported metal catalysts, alkaline modifiers are widely used as promoters of platinum group metal catalysts for many reactions [9–18]. It is widely recognized that the electron density of a supported noble metal is increased by the addition of alkaline and alkaline earth metals [14–18]. Although fundamental studies on the alkali-promotion effects have been important topics in heterogeneous catalysis, previous studies have focused on conventional reactions such as hydrogenolysis [10,11], oxidation [12,17,18], water gas shift reaction [13], and hydrogenation [14–16]. On the basis of the previous reports by Yoshitake and Iwasawa [14–16] that Na addition on Pt/SiO_2 increased electron density of Pt, we hypothesized that Na-loaded Pt/SiO_2 is a suitable material to discuss the electronic effect on the activity of Pt nanoparticle catalysts for one-pot green organic synthesis.

Amines are intermediates and products of enormous importance for chemical and life science applications. Pd- and Cu-catalyzed aminations of aryl halides [19] and the transition-metal-catalyzed amination of alcohols [20,21] represent attractive approaches for the alkylation of amines. The transition-metal-catalyzed alkylation of amines by amines is an attractive alternative method of alkylamine synthesis [22,29]. The reaction proceeds thorough a hydrogen-borrowing (hydrogen auto-transfer) mechanism [20,22–25]. The process begins with the dehydrogenation of an alkylamine to the corresponding imine. The imine undergoes addition of another nucleophilic amine and elimination of ammonia to form an *N*-alkyl imine, which is hydrogenated by in situ formed hydride species to the secondary amine product. Beller's Ru complexes [23,24] and Williams's Ir complexes [25] are successful

* Corresponding author. Tel.: +81 11 706 9240; fax: +81 11 706 9163.
E-mail address: kshimizu@cat.hokudai.ac.jp (K.-i. Shimizu).

1381-1169/$ – see front matter © 2011 Elsevier B.V. All rights reserved.
doi:10.1016/j.molcata.2011.11.021

Table 1
List of catalysts.

Catalysts	Na/Pt ratio	T_{cal}/°C[a]	T_{H_2}/°C[b]	D_{CO}/nm[c]	D_{TEM}/nm[d]
Pt/SiO_2	0	550	500	2.9	3.3
$NaPt/SiO_2$-0.2	0.2	500	200	3.0	–
$NaPt/SiO_2$-1	1	–	400	3.5	2.6
$NaPt/SiO_2$-2	2	–	300	3.1	–
$NaPt/SiO_2$-5	5	–	200	3.2	–
$NaPt/SiO_2$-10	10	–	200	3.3	2.4

[a] Temperatures of calcination.
[b] Temperatures of reduction in H_2.
[c] Average particle size of Pt estimated by CO adsorption experiment.
[d] Average particle size of Pt estimated by TEM.

catalytic systems for selective amine cross-coupling of different amines, leaving ammonia as the only by-product. From the environmental and economic viewpoints, it is preferable to accomplish the selective cross-coupling reaction using heterogeneous catalysts. Previous examples of Pt- and Pd-based heterogeneous systems for amine cross-coupling suffer from low selectivity for cross-coupling of different amines [26], reusability, low turnover number (TON), and need of stoichiometric amount of additives [29] or special reaction methods (microwave heating [29,30], electrocatalysis [27], photocatalysis [28]). In this paper, we found that Na-loaded Pt/SiO_2 showed higher turnover frequency (TOF), defined as the activity per unit of exposed metal surface, than Pt/SiO_2. Combined with various characterization results, the promoting effect of Na is discussed in terms of the support ionicity (electron density of support oxygen) and electron density of Pt, and a catalyst design concept is proposed.

2. Experimental

Commercially available organic compounds (from Tokyo Chemical Industry or Kishida Chemical) were used without further purification. The GC (Shimadzu GC-14B) and GCMS (Shimadzu GCMS-QP5000) analyses were carried out with a Rtx-65 capillary column (Shimadzu) using nitrogen as the carrier gas.

SiO_2-supported Pt (Pt/SiO_2 with Pt loading of 5 wt.%) was prepared by impregnating SiO_2 (Q-10, 300 $m^2\,g^{-1}$, supplied from Fuji Silysia Chemical Ltd.) with an aqueous HNO_3 solution of $Pt(NH_3)_2(NO_3)_2$ (Tanaka Kikinzoku), followed by evaporation to dryness at 80 °C, drying at 120 °C for 12 h, calcination in air at 500 °C, and reduction in a flow of 100% H_2 at 550 °C for 10 min. Sodium-loaded Pt/SiO_2 catalysts were prepared by impregnating Pt/SiO_2 with aqueous solution of $NaNO_3$, followed by evaporation to dryness at 80 °C, drying at 120 °C for 12 h, and reduction in a flow of H_2 for 10 min. To prepare a series of catalyst with different Na/Pt ratios but with similar Pt particle size, temperatures of reduction (T_{H_2}) were changed as summarized in Table 1. The catalysts are designated as $NaPt/SiO_2$-*x*, where *x* is the Na/Pt ratio. $NaPt/SiO_2$-2 was used as a standard catalyst.

The number of surface Pt atom in the Pt catalysts, pre-reduced in H_2 at 200 °C, was estimated with the CO uptake of the samples using the pulse-adsorption of CO in a flow of He. The average particle size was calculated from the CO uptake assuming that CO was adsorbed on the surface of semi-spherical Pt particles at CO/(surface Pt atom) = 1/1 stoichiometry.

Pt L_3-edge in situ XAFS measurement was carried out at BL01B1 of SPring-8 (Hyogo, Japan). The storage ring energy was operated at 8 GeV with a typical current of 100 mA. A self-supported wafer form (pressed pellet) of the pre-reduced Pt catalyst with 10 mm diameter was placed in a quartz in situ cell in a flow of 100% H_2 (100 $cm^3\,min^{-1}$) for 10 min at 200 °C under atmospheric pressure, and the sample was cooled to 40 °C under a flow of He, then the spectra were recorded in situ. The analyses of the extended X-ray absorption fine structure (EXAFS) and X-ray absorption near-edge structures (XANES) were performed using the REX version 2.5 program (RIGAKU). For EXAFS analysis, the spectra were extracted by utilizing the cubic spline method and normalized to the edge height. The Fourier transformation of the k^3-weighted EXAFS from *k* pace to *R* space was carried out over the *k* range 3.3–14.3 $Å^{-1}$ to obtain a radial distribution function. The inversely Fourier filtered data (in the *R* range of 1.5–3.3 Å) were analyzed with a usual curve fitting method in the *k* range of 3.3–14.3 $Å^{-1}$ using the empirical phase shift and amplitude functions for Pt–Pt and Pt–O shells extracted from the data for Pt foil and PtO_2, respectively. During the fitting procedure the absorber–scatterer distances, Debye–Waller factors or the coordination numbers were refined using a least squares refinement procedure.

Transmission electron microscopy (TEM) measurements were investigated using a JEOL JEM-2100F TEM operated at 200 kV.

The X-ray photoelectron spectroscopy (XPS) measurements were carried out using a JEOL JPS-900MC with Al Kα anode operated at 20 W and 10 kV. The oxygen 1s core electron levels in support oxides were recorded. Binding energies were calibrated with respect to C 1s at 285.0 eV.

In situ FTIR spectra were recorded at room temperature on a JASCO FT/IR-620 equipped with a quartz IR cell connected to a conventional flow reaction system. The sample was pressed into a 10 mg of self-supporting wafer and mounted into the quartz IR cell with CaF_2 windows. Spectra were measured accumulating 15 scans at a resolution of 4 cm^{-1}. A reference spectrum of the catalyst wafer in He was subtracted from each spectrum. Prior to each experiment the catalyst disk was heated in H_2 (2%)/He flow (100 $cm^3\,min^{-1}$) at temperatures shown in Table 1 for 10 min, followed by cooling to room temperature under He flow. Then, the catalyst was exposed to a flow of CO (0.9%)/He for 180 s.

$NaPt/SiO_2$-2 (1 mol.% Pt with respect to aniline) were added to the mixture of aniline (1.0 mmol), di-*iso*-propylamine (2.0 mmol) and *o*-xylene (2 mL) in a reaction vessel equipped with a condenser and N_2 was filled. Note that the aniline/di-*iso*-propylamine ratio of 2 was adopted because the reaction rate increased with the ratio as shown in Fig. 5. The resulting mixture was vigorously stirred under reflux condition (heating temperature = 155 °C) for 4 h. The reaction mixture was analyzed by GC. Conversion of aniline and yields of products were determined by GC using *n*-dodecane as an internal standard.

3. Results and discussion

3.1. Characterization

X-ray diffraction (XRD) pattern of $NaPt/SiO_2$-*x* (*x* = 0, 0.2, 1, 2, 5, 10) catalysts showed lines assignable to Pt metal (not shown). The number of surface metallic Pt atoms in these catalysts was estimated by the CO adsorption method, and the average size of metallic Pt particles was estimated by assuming that CO was adsorbed on the surface of semi-spherical Pt particles at CO/(surface Pt atom) = 1/1 stoichiometry. As summarized in Table 1, the Pt particle sizes, which did not markedly depend on the Na/Pt ratio, were in a range of 2.9–3.5 nm. The average Pt particle size of selected samples, $NaPt/SiO_2$-*x* (*x* = 0, 1, 10), was estimated from TEM analysis. As listed in Table 1, the particle size of these samples did not markedly depend on the Na/Pt ratio, but slightly decreased with the Na/Pt ratio. The Pt particle sizes from TEM (2.4–3.3 nm) were approximately close to those from CO adsorption. However, it should be noted that the particle size for Pt/SiO_2 from TEM (3.3 nm) is slightly larger than that from CO adsorption (2.9 nm), while those for $NaPt/SiO_2$-1 (2.6 nm) and $NaPt/SiO_2$-10 (2.4 nm) from TEM are slightly smaller than those from CO adsorption (3.5 and 3.3 nm). Considering a generally observed tendency that the

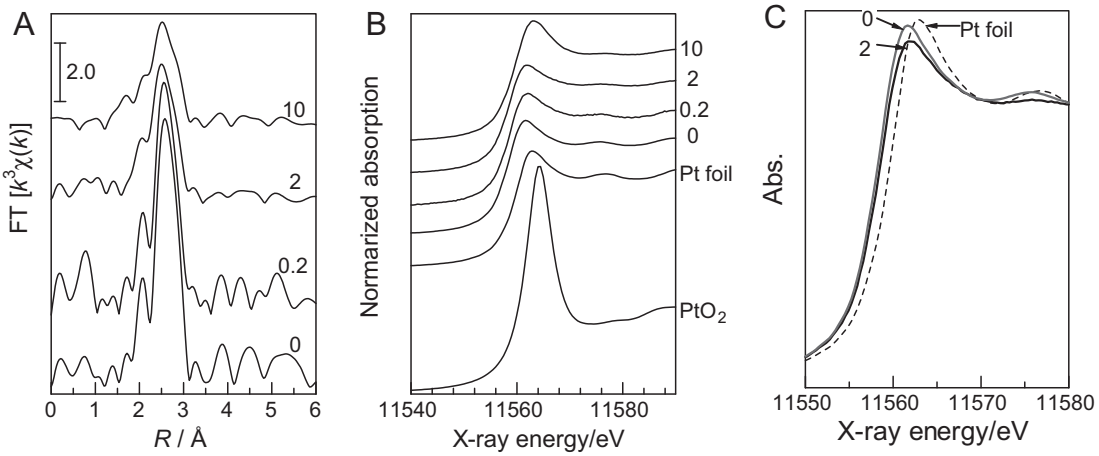

Fig. 1. (A) EXAFS Fourier transforms and (B and C) XANES spectra at Pt L_3-edge for $NaPt/SiO_2$-*x* recorded in situ under He at 40 °C after flowing H_2 for 10 min at 200 °C. Na/Pt ratio (*x*) of the catalyst is shown in the figure. Ex situ XANES spectra of reference Pt compounds are included in (B) and (C).

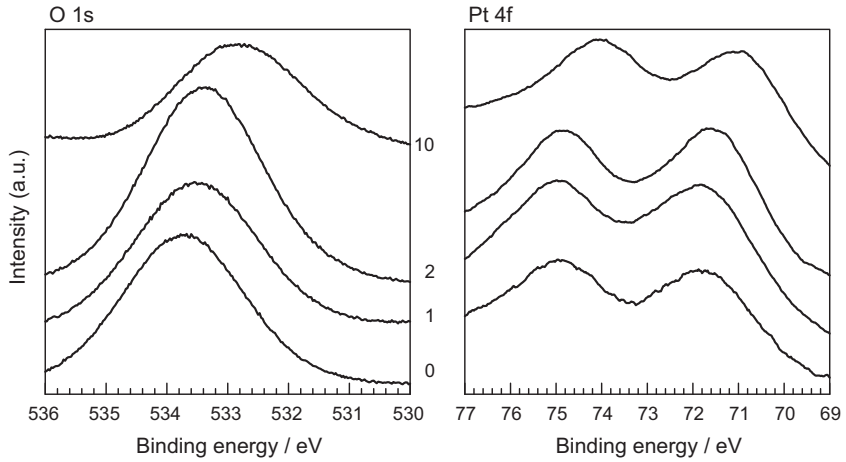

Fig. 2. XPS spectra of the O 1s and Pt 4f regions of $NaPt/SiO_2$-*x*. Na/Pt ratio (*x*) of the catalyst is shown in the figure.

Table 2
Curve-fitting analysis of Pt L_3-edge in situ EXAFS.

Sample	Shell	*N*[a]	*R*/Å[b]	(*σ*)/Å[c]	R_f (%)[d]
Pt/SiO_2	Pt	10.6	2.75	0.083	0.9
$NaPt/SiO_2$-0.2	Pt	9.6	2.74	0.086	0.7
$NaPt/SiO_2$-2	Pt	8.0	2.71	0.096	1.1
$NaPt/SiO_2$-10	Pt	7.1	2.72	0.089	1.0
	O	0.7	1.93	0.089	

[a] Coordination numbers.
[b] Bond distance.
[c] Debye–Waller factor.
[d] Residual factor.

average particle size from TEM is larger than that from CO adsorption, this result suggests that the surface of metallic Pt particles in Na-loaded samples are partially covered with Na species.

Fig. 1A shows k^3-weighted in situ extended X-ray absorption fine structure (EXAFS) data of $NaPt/SiO_2$-*x* catalysts acquired at room temperature in a flow of He after H_2-reduction at 200 °C. The values of the coordination numbers for Pt–O and Pt–Pt species as well as the distances (EXAFS analysis) are included in Table 2. The analysis of the spectra reveals metallic Pt signatures. The EXAFS of $NaPt/SiO_2$-*x* consists of a Pt–Pt contribution with coordination number of 7.1–10.6 at bond distance of 2.71–2.75 Å. A weak Pt–O contribution observed for $NaPt/SiO_2$-10 may be assigned to Pt–O–Na bond, because this feature was not observed for the catalysts with low Na coverage. The Pt–Pt coordination number decreased with increase in the Na/Pt ratio. This suggests that Pt particle size decreases with Na loading, which is consistent with the trend from the TEM results, but such trend is not observed from the CO adsorption experiments (Table 1). These results suggest that the surface of metallic Pt particles in Na-loaded catalysts is partially covered with NaO_x species. This model is consistent with that proposed by Yoshitake and Iwasawa [15] for Na-loaded Pt/SiO_2 catalysts pre-reduced at 200 °C before various characterization experiments. Partial covering of Pt surface by NaO_x has been recently reported by Mallinson and co-workers in their detailed structural study of Na-promoted Pt/TiO_2 catalyst [13]. Using high resolution TEM, they showed that the Pt particles were partially covered by NaO_x. For K-loaded Pt/Al_2O_3, Busca et al. also have proposed that Pt centers lie in close proximity of potassium oxide species [9].

To estimate electronic effect of Na-addition on the electronic states of the support, we measured the binding energy (BE) of the O 1s electron in the support oxide by XPS analysis. It is established that the O 1s binding energy of metal oxides decreases with increase in the electron density of oxygen in the metal oxide, or in other words, ionicity of the metal oxide [11]. XPS spectra of the O 1s region in the supports are given in Fig. 2. The O 1s BE decreased with an increase in the Na/Pt ratio, indicating that the electron charge of the support oxygen atoms increased with the amount of electropositive modifier (Na). This result was consistent with that reported by

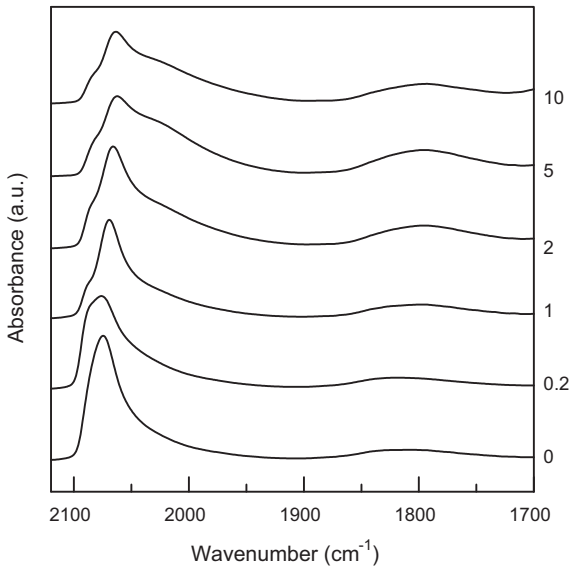

Fig. 3. FTIR spectra of CO adsorbed on $NaPt/SiO_2$-*x*. Na/Pt ratio (*x*) of the catalyst is shown in the figure.

Koningsberger and co-workers [11], in which they observed that the O 1s BE of the Al_2O_3 support systematically decreased with decrease in the electronegativity of alkaline modifiers.

The XPS spectra in the region of the Pt $4f_{7/2}$ are also shown in Fig. 2. The Pt $4f_{7/2}$ BE of unmodified Pt/SiO_2 catalyst (71.9 eV) was in between those of Pt^{2+} (72.6 eV) and Pt^0 (71.1 eV) [13]. Although the catalysts were reduced as shown in Table 1, the re-oxidation of Pt by O_2 in air should result in the formation of cationic Pt species on the surface. The increase in the Na/Pt ratio caused the negative shift of the Pt $4f_{7/2}$ BE for $NaPt/SiO_2$-*x* catalysts, and the BE of $NaPt/SiO_2$-10 (71.0 eV) was lower than that of Pt^0 (71.1 eV). This result indicates that electron charge of the Pt atoms increases as the amount of electropositive modifier (Na) increases. This conclusion is supported by in situ X-ray absorption near-edge structures (XANES) spectra of $NaPt/SiO_2$-*x* measured at 40 °C in a flow of He after reduction at 200 °C in H_2 (Fig. 1B). It is established that Pt L_3-edge XANES spectrum is sensitive to the oxidation state of Pt; the absorption peak around 11,564 eV (white line) increases with increase in the oxidation number of Pt. The white line intensity of $NaPt/SiO_2$-2 is lower than that of $NaPt/SiO_2$-0, which indicates that the presence of Na on Pt/SiO_2 increases the electron density of metallic Pt. In situ XANES reflects the changes in the average oxidation states of Pt located at bulk and surface of metal particles. IR spectroscopy with CO as a probe molecule allows monitoring of the changes in the electronic states of surface Pt. Fig. 3 shows IR spectra of CO adsorbed on $NaPt/SiO_2$-*x* catalysts. It is widely recognized that the wavenumber of CO stretching increases with an increase in the electron deficiency of the metal [10–12,17,18]. In a region characteristic to linearly coordinated CO on metallic Pt (2100–2000 cm^{-1}), the wavenumber of the maximum intensity decreased with the Na/Pt ratio, suggesting an increase in the electron density of Pt [9]. Similar results were recently reported by Busca et al. [9] for CO adsorption IR study of K-loaded Pt/Al_2O_3, in which they showed that the presence of K on Pt/Al_2O_3 increased the basicity of the catalysts and consequently increased the electron density of Pt, as evidenced by the lower CO stretching frequency of CO on Pt. In addition, the relative intensity of the bridge-bonded CO band at 1800 cm^{-1} as compared to the linear-CO band increased with the Na/Pt ratio. This trend is similar to those reported for alkali cation promoted Pt and Rh catalyst [10,11,17,18]. There is a general trend that the ratio of bridging bonded to linear bonded CO (B/L) increases with increase in electron density of metal particle.

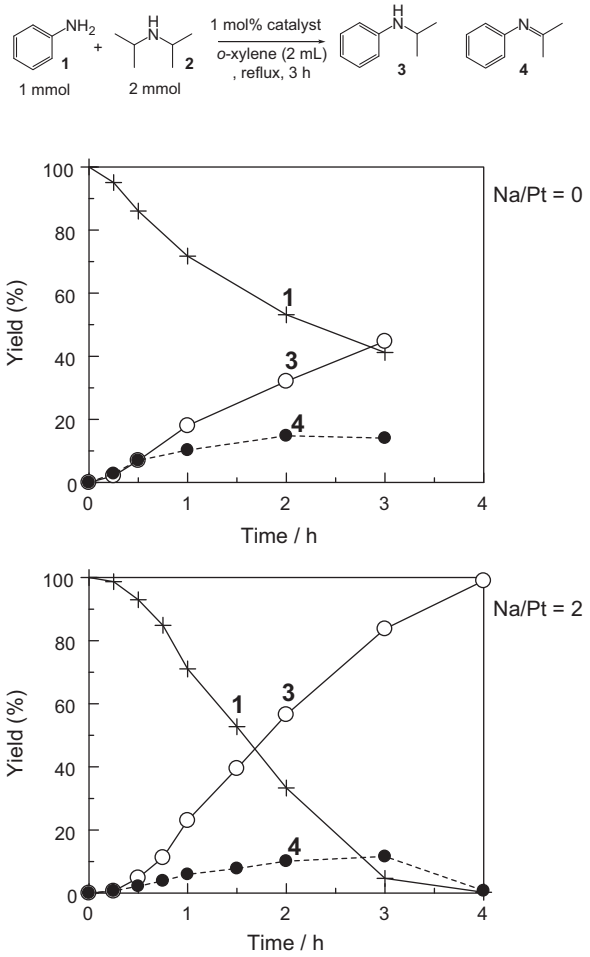

Fig. 4. Yields of (+) **1**, (○) **3** and (●) **4** for the reaction of aniline with iPr_2NH by (top) Pt/SiO_2 and (bottom) $NaPt/SiO_2$-2 vs. reaction time.

The group of Weckhuysen [17,18] reported systematic IR studies of CO adsorption on alkali cation exchanged Y zeolite-supported Pt and Rh catalysts and reported that the B/L ratio increased with a decrease in the electronegativity of alkaline cation. The group of Koningsberger and co-workers [10,11] also showed that as the electronegativity of alkaline cations added in Pt/Al_2O_3 decreased, the electron charge in the support oxides increased (O 1s BE of the support decreased) and consequently increase in the electron density of Pt particle (increase in B/L ratio) [11]. It has been explained that more electropositive cations are pushing toward the oxygen atoms of the support and this causes the Pt metal particles to have a higher electron density. From the above discussion, it can be concluded that that electron charge of the Pt metal particles increases as the amount of electropositive modifier (Na) increases as a result of the increased electron charge of the oxygen atoms on the support. In addition to this indirect electron transfer from Na to Pt via the oxygen atoms of the support, the increase in the electron density of the Pt metal particles may be partly attributed to the direct electron donation form Na to the Pt metal particles.

3.2. Catalytic and kinetic studies

As shown in the above section, the SiO_2-supported Pt metal catalysts with different Na/Pt ratios *x* (*x* = 0, 0.2, 1, 2, 5, 10) but with the similar Pt metal particle size were prepared, and the electron charge of the Pt metal particles increased with the Na/Pt ratio. As a test reaction of cross-coupling reaction of amines, we examined *N*-alkylation of aniline (**1**) with 2 equiv. of di-*iso*-propylamine

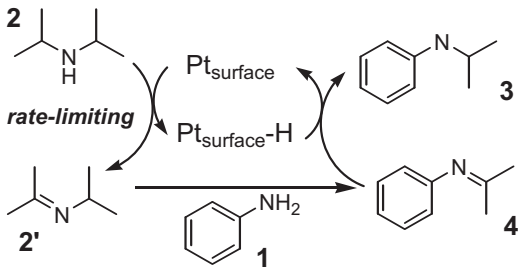

Scheme 1. Mechanism of Pt-catalyzed alkylation of aniline with iPr$_2$NH. Pt$_{surface}$ represents metallic Pt sites on the surface of Pt nanoparticle.

(**2**), iPr$_2$NH, under o-xylene reflux condition in N_2 atmosphere in the presence of NaPt/SiO$_2$-x (1 mol.% of Pt with respect to **1**). Fig. 4 shows changes in the yields of the unreacted aniline **1**, an imine intermediate (isopropylidene-phenylamine **4**) and a desired hydrogenated product (*N*-isopropylaniline **3**) which can be produced by the reduction of **4**. In the presence of NaPt/SiO$_2$-2, a typical time-conversion profile of the consecutive reaction was observed; the imine intermediate **4**, formed at an initial period, was consumed, and then yield of the hydrogenated product **3** increased with time. After 4 h, conversion of aniline **1** reached 100% and the desired amine **3** was obtained in 99% yield, while the yield of **4** was below 1%. It should be noted that the turnover frequency (TOF) based on the total Pt content is 24.7, which is higher than that of homogeneous Ir catalyst (TOF = 9.8) [25] for the same reaction at the same temperature. This demonstrates a highly efficient feature of the present catalytic system.

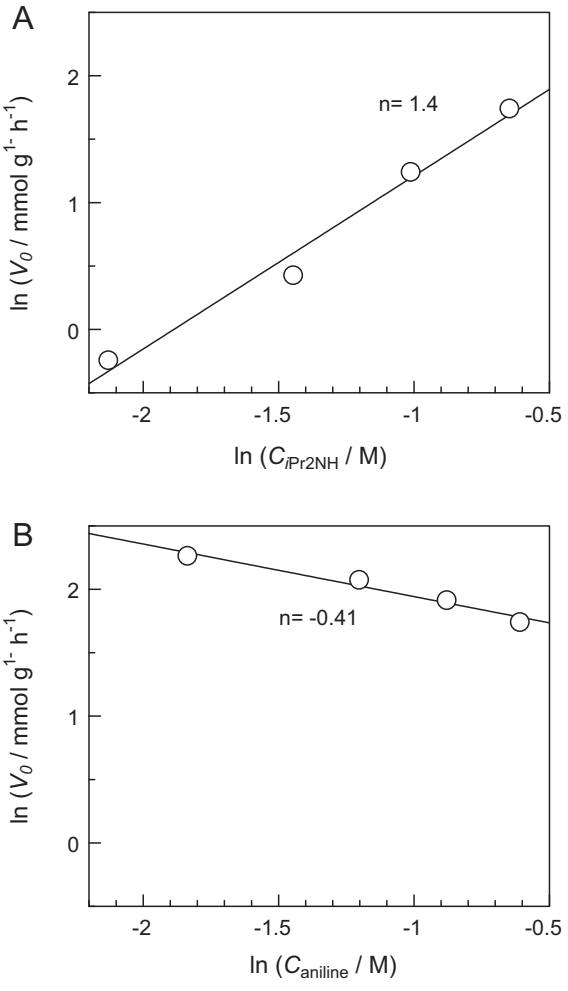

Fig. 5. Formation rate of **3** (○) as a function of the concentration of (A) iPr$_2$NH and (B) aniline for the reaction of aniline with iPr$_2$NH by NaPt/SiO$_2$-2.

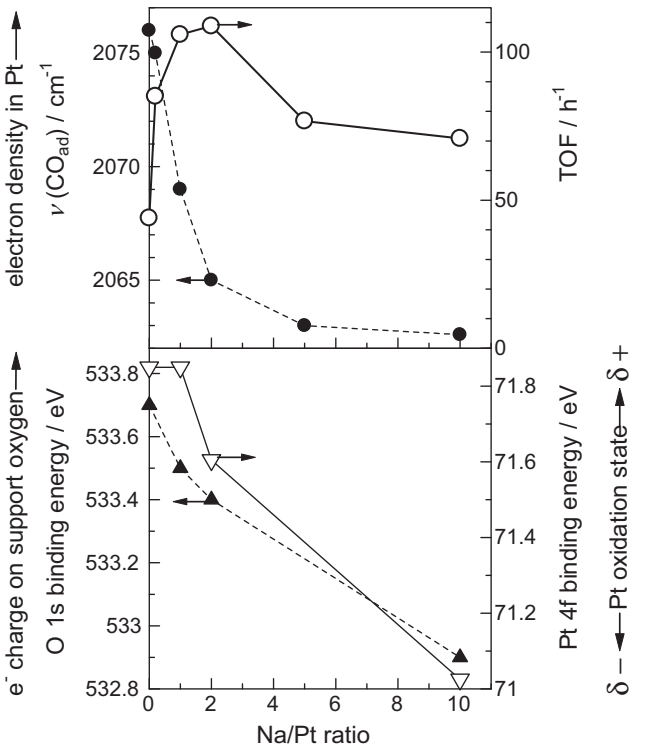

Fig. 6. Effect of Na/Pt ratio in NaPt/SiO$_2$-x catalysts on (▲) O 1s binding energy, Pt 4f binding energy and (▽), IR band position of the linear coordinated CO (●), and (○) TOF based on the number of surface Pt atom.

As previously postulated by the group of Murahashi et al. [22], Beller [23,24] and Williams [25], it is most probable that the amine cross-coupling reaction proceeds through the hydrogen borrowing pathway (Scheme 1), in which the reaction is initiated by a temporary removal of hydrogen from iPr$_2$NH **2** to generate imine **2**′ and Pt–H species. The following kinetic results give further evidences on the mechanism for the Pt-catalyzed *N*-alkylation of aniline **1** with iPr$_2$NH **2**. As mentioned above, the kinetic curve for NaPt/SiO$_2$-2 (Fig. 4) indicates that *N*-isopropylaniline **3** is produced through a consecutive pathway via the *N*-alkylimine **4**. Since the reaction was performed under N_2, it is reasonable to assume that imine **4** was hydrogenated by hydrogen species in situ formed on dehydrogenation of iPr$_2$NH. The effect of reactant concentration on the activity was tested for NaPt/SiO$_2$-2. In Fig. 5, the reaction rates are plotted as a function of the initial concentration of iPr$_2$NH and aniline. The rate of **3** formation increased with the initial iPr$_2$NH concentration, which corresponds to the reaction order (n) of 1.4 (Fig. 5A). The rate dependence on the aniline concentration (Fig. 5B) showed a negative order dependence ($n = -0.40$). These results suggest that iPr$_2$NH is involved in a rate-limiting step and aniline is not involved in the rate-limiting step. The results also rule out the hydrogenation of imine **4** by Pt–H species to regenerate Pt site as rate determining step. The negative-order for aniline suggests that strong adsorption of aniline on the surface active site inhibits the catalytic reaction. The above results support a possible reaction mechanism in Scheme 1. The reaction begins with the dehydrogenation of an alkylamine to the corresponding imine as the rate-limiting step. The imine undergoes fast addition of aniline and elimination of ammonia to form an *N*-alkylimine, which is hydrogenated by in situ formed Pt–H species to the secondary amine product.

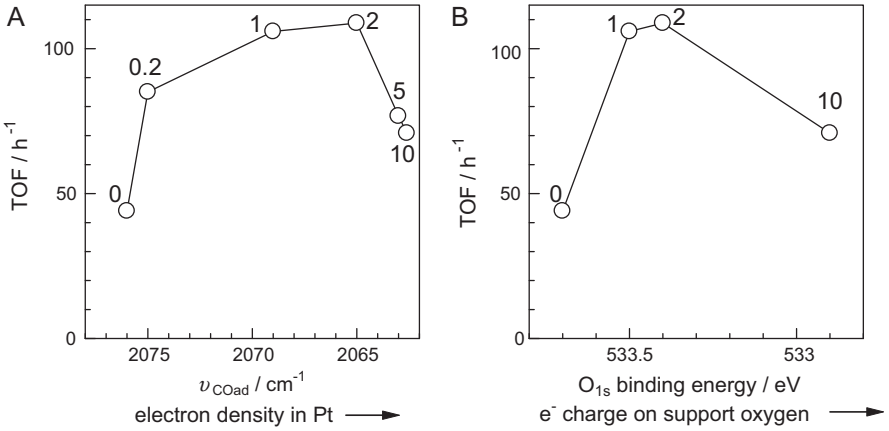

Fig. 7. Effect of (A) IR band position of the linear coordinated CO and (B) O 1s biding energy on the catalytic activity (TOF based on the number of surface Pt atom) of $NaPt/SiO_2$-*x*. Na/Pt ratio (*x*) of the catalyst is shown in the figures.

3.3. Structure–activity relationship

In contrast to $NaPt/SiO_2$-2, the unmodified Pt/SiO_2 catalyst showed lower yield of **3**, while it showed slightly higher yield of **4** than $NaPt/SiO_2$-2 (Fig. 4). Note that Pt-free catalyst with the same Na loading (Na/SiO_2) showed no activity after 4 h. The rate of **3** formation was also measured under the condition where conversion of aniline was below 50%, and TOF based on the surface Pt atoms was calculated using the reaction rate and the number of surface Pt atoms (from CO adsorption experiment). It is found that TOF for $NaPt/SiO_2$-2 is larger than that for Pt/SiO_2 by a factor of 2.4. For a series of $NaPt/SiO_2$-*x* catalysts with different Na/Pt ratios but with the same Pt loading (5 wt.%) and similar Pt particle size (Table 1), shift of the linear-CO IR band, $\nu(CO_{ad})$ as an index of electron density of surface Pt, the catalytic activity (TOF), Pt $4f_{7/2}$ BE as an index of average oxidation state of Pt atoms at the surface and near surface and O 1s BE as an index of the electron charge of the support oxygen atoms are plotted as a function of Na/Pt ratio in Fig. 6. TOF showed a volcano-type dependence on the Na/Pt ratio, and $NaPt/SiO_2$-2 showed the highest reaction rate (TOF). To discuss the effect of electronic effects of Na on the catalytic activity, TOF are plotted as a function of $\nu(CO_{ad})$ and the O 1s BE of the support oxides (Fig. 7). In both cases, TOF shows volcano-type dependence on $\nu(CO_{ad})$ and the O 1s BE with the maximum activity in a Na/Pt range of 1–2. The results suggest that a moderate electron charge of the support oxygen atom causes a moderate electron density of Pt metal particles, which results in the high activity.

The effect of alkaline modifier on the electronic properties of Pt particles has been investigated by Koningsberger and co-workers, using experimental (XAFS) and DFT calculations [10,11]. For hydrogen adsorption on K doped Pt/Al_2O_3, they concluded that the Pt–H bond strength increases with ionicity (basicity) of the support oxide [11]. They proposed that the shift in the Pt 6s and p and 5d orbitals upon interaction with the support is the origin of the higher Pt–H bond strength on the ionic (basic) support. This model has explained why Pt on acidic (less ionic) support gave higher activity in hydrogenolysis and hydrogenation reactions; the less stable Pt–H species has higher reactivity [10]. Taking this trend into account, we propose the following hypotheses on a possible role of ionicity of the support on the catalytic activity and selectivity. Pt metal particles on less ionic support have relatively low electron density and consequently weak Pt–H bond. According to linear free energy (Brønsted–Evans–Polanyi) relationships widely observed in heterogeneous catalysis, the weak Pt–H bond should result in the low activity for the C–H bond dissociation of iPr_2NH as the rate-limiting step of the catalytic cycle. In contrast, the Pt–H bond on basic support is too stable, and hydrogenation of **4** to **3** by Pt–H is slow, which results in low rate of H removal from Pt sites to regenerate coordinatively unsaturated Pt sites. Therefore, $NaPt/SiO_2$-2 with moderate electron density in Pt shows the highest rate of **3** formation. Another possible explanation on the support dependent activity and selectivity may be based on metal-support bi-functional mechanism, where acid–base sites on the support take part in a certain step of the catalytic cycle. Basic sites of the support may play a role in C–H abstraction of iPr_2NH, and acid sites may be effective for a polarization C=N bond of imine and thus promote hydrogenation of imine.

4. Conclusions

For the catalytic mono-*N*-alkylation of aniline with iPr_2NH, addition of moderate amount of Na (Na/Pt ratio of 2) enhanced the catalytic activity (TOF) of Pt/SiO_2 by a factor of 2.4. TOF showed a volcano type dependence on the Na/Pt ratio, and the catalyst with the Na/Pt ratio of 2 showed the highest TOF. The Na/Pt ratio affected the electronic states of the support oxide and Pt; increase in the Na/Pt ratio increased the electron density of the oxygen atom of support oxides and consequently increased the electron density of Pt metal. The reaction proceeds through the hydrogen-borrowing mechanism including the formation and reaction of Pt–H species. The high catalytic activity of the catalyst with moderate electron density of Pt could be due to a moderate stability of Pt–H species.

Acknowledgments

This work was supported by the Japanese Ministry of Education, Culture, Sports, Science and Technology via Grant-in-Aids for Scientific Research B (20360361) and for Young Scientists A (22686075). The X-ray absorption experiment was performed with the approval of the Japan Synchrotron Radiation Research Institute (Proposal No. 2010B1447).

Appendix A. Supplementary data

Supplementary data associated with this article can be found, in the online version, at doi:10.1016/j.molcata.2011.11.021.

References

[1] K. Yamaguchi, N. Mizuno, Synlett (2010) 2365–2382.
[2] K. Kaneda, T. Mizugaki, Energy Environ. Sci. 2 (2009) 655–673.
[3] M.J. Climent, A. Corma, S. Iborra, Chem. Rev. 111 (2011) 1072–1133.

[4] K. Shimizu, K. Satwabe, A. Satsuma, Catal. Sci. Technol. 1 (2011) 331–341.
[5] N. Toshima, Y. Shiraishi, T. Teranishi, M. Miyake, T. Tominaga, H. Watanabe, W. Brijoux, H. Bönnemann, G. Schmid, Appl. Organomet. Chem. 15 (2001) 178–196.
[6] S. Ikeda, S. Ishino, T. Haranda, N. Okamoto, T. Sakata, H. Mori, S. Kuwabata, T. Torimoto, M. Matsumura, Angew. Chem. Int. Ed. 45 (2006) 7063–7066.
[7] Y.H. Ng, S. Ikeda, T. Harada, Y. Morita, M. Matsumura, Chem. Commun. (2008) 3181–3183.
[8] P. Mäki-Arvela, A.V. Tokarev, E.V. Murzina, B. Campo, T. Heikkilä, J.-M. Brozinski, D. Wolf, D. Yu Murzin, Phys. Chem. Chem. Phys. 13 (2011) 9268–9280.
[9] T. Montanari, R. Matarrese, N. Artioli, G. Busca, Appl. Catal. B 105 (2011) 15–23.
[10] M.K. Oudenhuijzen, J.A. van Bokhoven, J.T. Miller, D.E. Ramaker, D.C. Koningsberger, J. Am. Chem. Soc. 127 (2005) 1530–1540.
[11] A.Y. Stakheev, Y. Zhang, A.V. Ivanov, G.N. Baeva, D.E. Ramaker, D.C. Koningsberger, J. Phys. Chem. C 111 (2007) 3938–3948.
[12] Y. Yazawa, H. Yoshida, S. Komai, T. Hattori, Appl. Catal. A 233 (2002) 113–124.
[13] X. Zhu, M. Shen, L.L. Lobban, R.G. Mallinson, J. Catal. 278 (2011) 123–132.
[14] H. Yoshitake, Y. Iwasawa, J. Phys. Chem. 96 (1992) 1329–1334.
[15] H. Yoshitake, Y. Iwasawa, J. Catal. 131 (1991) 276–284.
[16] H. Yoshitake, Y. Iwasawa, J. Phys. Chem. 95 (1991) 7368–7372.
[17] T. Visser, T.A. Nijhuis, A.M.J. van der Eerden, K. Jenken, Y. Ji, W. Bras, S. Nikitenko, Y. Ikeda, M. Lepage, B.M. Weckhuysen, J. Phys. Chem. B 109 (2005) 3822–3831.
[18] M. Lepage, T. Visser, F. Soulimani, A.M. Beale, A. Iglesias-Juez, A.M.J. van der Eerden, B.M. Weckhuysen, J. Phys. Chem. C 112 (2008) 9394–9404.
[19] D. Maiti, B.P. Fors, J.L. Henderson, Y. Nakamura, S.L. Buchwald, Chem. Sci. 2 (2011) 57–68.
[20] G. Guillena, D.J. Ramon, M. Yus, Chem. Rev. 110 (2010) 1611–1641.
[21] T.D. Nixon, M.K.##J.M Whittlesey, J. Williams, Dalton Trans. (2009) 753–762.
[22] S.-I. Murahashi, T. Hirano, T. Yano, J. Am. Chem. Soc. 100 (1978) 348–350.
[23] D. Hollmann, S. Bahn, A. Tillack, M. Beller, Angew. Chem. Int. Ed. 46 (2007) 8291–8294.
[24] D. Hollmann, S. Bahn, A. Tillack, M. Beller, Chem. Commun. (2008) 3199–3201.
[25] O. Saidi, A.J. Blacker, M.M. Farah, S.P. Marsden, J.M.J. Williams, Angew. Chem. Int. Ed. 48 (2009) 7375–7378.
[26] N. Sivasankar, R. Prins, J. Catal. 241 (2006) 342–355;
A. Prades, R. Corberan, M. Poyatos, E. Peris, Chem. Eur. J. 14 (2008) 11474–11479.
[27] M. Largeron, M.-B. Fleury, Org. Lett. 11 (2009) 883–886.
[28] S.-I. Nishimoto, B. Ohtani, T. Yoshikawa, T. Kagiya, J. Am. Chem. Soc. 105 (1983) 7180–7182.
[29] A. Miyazawa, K. Saitou, K. Tanaka, T.M. Gädda, M. Tashiro, G.K.S. Prakash, G.A. Olah, Tetrahedron Lett. 47 (2006) 1437–1439.
[30] M.C. Lubinu, L.D. Luca, G. Giacomelli, A. Porcheddu, Chem. Eur. J. 17 (2011) 82–85.